PHILOSOPHICAL TRANSACTIONS OF THE ROYAL SOCIETY A MATHEMATICAL, PHYSICAL & ENGINEERING SCIENCES

Symmetry-extended counting rules for periodic frameworks

S. D. Guest and P. W. Fowler

Phil. Trans. R. Soc. A 2014 **372**, 20120029, published 30 December 2013

PHILOSOPHICAL TRANSACTIONS OF THE ROYAL SOCIETY A

rsta.royalsocietypublishing.org

Research

Cite this article: Guest SD, Fowler PW. 2014 Symmetry-extended counting rules for periodic frameworks. *Phil. Trans. R. Soc. A* **372**: 20120029.
http://dx.doi.org/10.1098/rsta.2012.0029

One contribution of 14 to a Theo Murphy Meeting Issue 'Rigidity of periodic and symmetric structures in nature and engineering'.

Subject Areas:
structural engineering, crystallography

Keywords:
frameworks, periodicity, symmetry

Author for correspondence:
S. D. Guest
e-mail: sdg@eng.cam.ac.uk

Royal Society Publishing

Symmetry-extended counting rules for periodic frameworks

S. D. Guest[1] and P. W. Fowler[2]

[1]Department of Engineering, University of Cambridge, Trumpington Street, Cambridge CB2 1PZ, UK
[2]Department of Chemistry, University of Sheffield, Sheffield S3 7HF, UK

A symmetry-adapted version of the Maxwell rule appropriate to periodic bar-and-joint frameworks is obtained, and is further extended to body-and-joint systems. The treatment deals with bodies and forces that are replicated in every unit cell, and uses the point group isomorphic to the factor group of the space group of the framework. Explicit expressions are found for the numbers and symmetries of detectable mechanisms and states of self-stress in terms of the numbers and symmetries of framework components. This approach allows detection and characterization of mechanisms and states of self-stress in microscopic and macroscopic materials and meta-materials. Illustrative examples are described. The notion of local isostaticity of periodic frameworks is extended to include point-group symmetry.

1. Introduction

Counting arguments give powerful conditions on rigidity/mobility of finite structures, and we consider here their applicability to extended periodic structures. Many objects in the macroscopic and microscopic worlds have been modelled as bar-and-joint frameworks, which consist of stiff bars connected with flexible joints (pin joints in two dimensions, spherical joints in three dimensions). Counting arguments for these frameworks were first formally expressed by Maxwell [1]. This rule, in the extension described by Calladine [2], is

$$\left.\begin{array}{lll} & \text{(two dimensions)} & m - s = 2j - b - 3 \\ \text{and} & \text{(three dimensions)} & m - s = 3j - b - 6, \end{array}\right\} \quad (1.1)$$

where m is the number of mechanisms, s the number of states of self-stress, j the number of joints and b the number of bars of the framework. In this formulation, the constant terms on the RHS account for the rigid-body motions of the unsupported framework.

Scalar counting rules of this kind are powerful but give limited information because they yield only the difference between the *numbers* of mechanisms and states of self-stress. The information content can be extended by considering the *symmetries* of the framework, and applying the counting approach symmetry by symmetry. Such an approach can reveal the existence of mechanisms and states of self-stress which are hidden by cancellation within the bare scalar count. These extensions can be written compactly in terms of (typically reducible) *representations* Γ(object) which collect the *characters* $\chi_{\text{object}}(S)$ of sets of objects. For each symmetry operation S, $\chi_{\text{object}}(S)$ is the trace of the matrix that relates the set before and after application of S. For frameworks, the key representations are $\Gamma(b)$ and $\Gamma(j)$, which describe the symmetries of bars and joints, respectively.

The symmetry-extended version of (1.1) is, from [3],

$$\Gamma(m) - \Gamma(s) = \Gamma(j) \times \Gamma_{\mathrm{T}} - \Gamma(b) - \Gamma_{\mathrm{T}} - \Gamma_{\mathrm{R}}, \tag{1.2}$$

where Γ_{T} and Γ_{R} are representations of relevant rigid-body translations and rotations, respectively. They are

$$\left.\begin{array}{lll} & \text{(two dimensions)} & \Gamma_{\mathrm{T}} = \Gamma(T_x, T_y); \quad \Gamma_{\mathrm{R}} = \Gamma(R_z) \\ \text{and} & \text{(three dimensions)} & \Gamma_{\mathrm{T}} = \Gamma(T_x, T_y, T_z); \quad \Gamma_{\mathrm{R}} = \Gamma(R_x, R_y, R_z), \end{array}\right\} \tag{1.3}$$

where the two-dimensional restriction is to the (x, y) plane. A similar development can be framed for other models of structures: a finite body-and-joint framework also has a scalar counting rule for net mobility [4,5], and a symmetry extension of this counting rule has been derived [6].

Scalar counting can also be extended to periodic structures defined by a representative unit cell. This formulation, and its further extension to include symmetry, are the topics of this paper. We show how the extended equations can be constructed for both pin-jointed and body-joint frameworks and give some examples of their use. For pin-jointed periodic frameworks, Ross *et al.* [7] and Malestein & Theran [8] have previously considered counting for systems that are constrained to retain certain symmetries. Here, within a chosen periodicity, we effectively provide counts for all possible symmetries.

2. Counting for periodic bar-and-joint structures

The basis of our approach is the consideration of the displacement and forces within the unit cell. The complete infinite structure is considered by translations of this cell. It is assumed here that the behaviour of the contents of the cell is also replicated by translation, i.e. we work in the $k = 0$ wavevector regime [9]. For these assumptions, Borcea & Streinu [10] give the extension of the scalar Maxwell counting rule for periodic structures. Here, we give an alternative derivation that provides a basis for the further extension to include symmetry as described in §3.

A key element of the extension of rules (1.1) and (1.2) to repetitive periodic frameworks is the consideration of the appropriate rigid-body motions and deformations of the unit cell. Consider initially the affine infinitesimal deformations of a unit cell, used in solid mechanics to provide a basis for the strain tensor [11]. One basis for all possible deformations of the two-dimensional unit cell (i.e. excluding rigid-body translations and rotations) is the set of the two orthogonal stretches in x- and y-directions, and the single xy shear (figure 1). In three dimensions, a suitable basis for the possible deformations of the unit cell is the set of three orthogonal stretches (in x-, y- and z-directions) and three shears (xy, yz, zx).

In periodic systems, the freedoms of the joints comprise the freedoms of each joint within the representative unit cell *plus* the deformations of the unit cell itself. Thus, the count of freedoms in two dimensions is $2j + 3$, and in three dimensions is $3j + 6$. However, this freedom includes rigid-body motions (two in two dimensions and three in three dimensions) that we wish to exclude

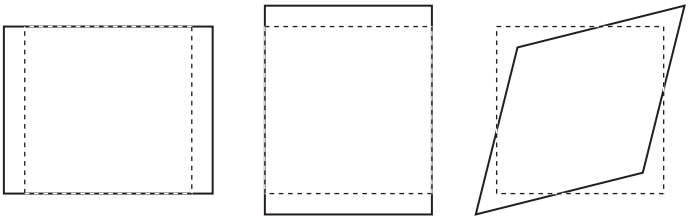

Figure 1. The deformations of the unit cell that are compatible with periodic mobility in two dimensions, comprising (left to right) two orthogonal stretches and one shear.

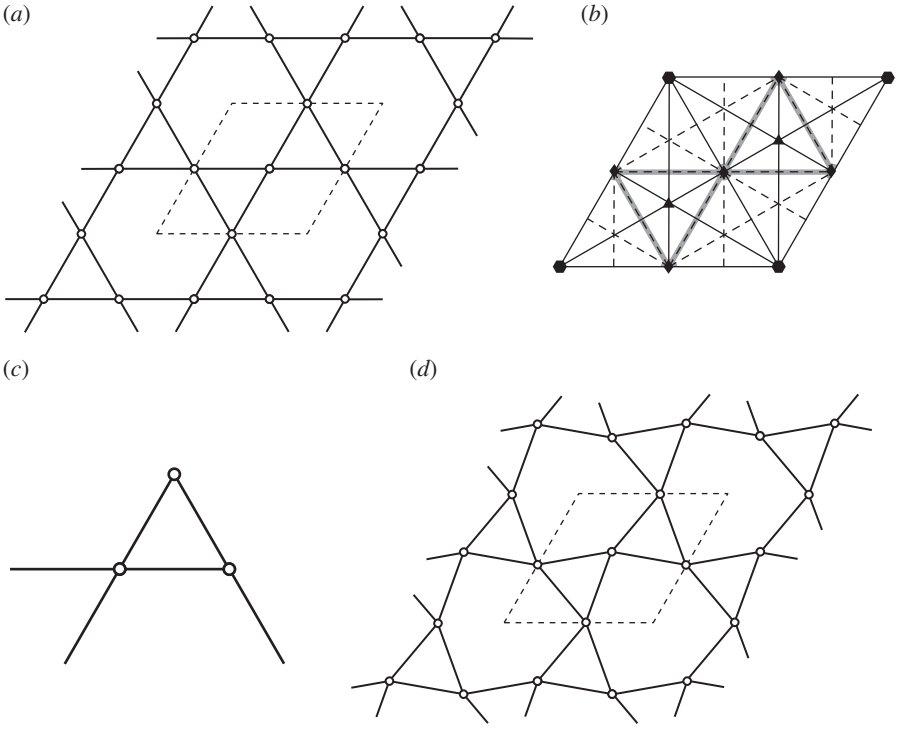

Figure 2. The kagome framework. (*a*) The choice of unit cell used here; (*b*) the unit cell with symmetry elements denoted by the standard symbols of a rhombus for a C_2 axis, triangle for a C_3 axis, hexagon for a C_6 axis, solid line for a reflection line, and a dashed line for a glide line; (*c*) a motif with a minimal set of complete joints and bars; and (*d*) a deformed configuration, illustrating the B_2-symmetric mechanism detected by the analysis reported in §4*a*.

from the list of mechanisms. Hence, the periodic equivalent of (1.2) is

$$\left.\begin{aligned} &\text{(two dimensions)} \quad m - s = 2j - b + 3 - 2 = 2j - b + 1 \\ \text{and} \quad &\text{(three dimensions)} \quad m - s = 3j - b + 6 - 3 = 3j - b + 3. \end{aligned}\right\} \tag{2.1}$$

The RHS of (2.1) differs from the finite case (1.1) by addition of counts of four (two dimensions) and nine (three dimensions), respectively. These equations can be derived more formally by considering the dimensions of the augmented compatibility matrix as described by Guest & Hutchinson [12].

A simple example system to illustrate the application of (2.1) is the kagome framework shown in figure 2. With the given choice of smallest unit cell, $j = 3$ and $b = 6$, where two of the joints lie on the unit cell boundary. The figure also shows what Owen & Power [13] call a 'motif', made up of complete joints and bars, disjoint copies of which recover the full kagome lattice by translation.

Except for systems which are *locally isostatic* [14], the result for $m - s$ obtained from (2.1) will depend on the size of the unit cell chosen. Choosing a unit cell that is larger than the minimum unit cell effectively allows additional wavevectors to be considered, beyond a $k = 0$ wavevector regime based on the minimum unit cell.

3. Counting with symmetry for periodic bar-and-joint structures

The symmetry group $\mathcal{G}$ that describes a periodic framework is a *space group* (or, in two dimensions, a *plane group*). We consider the extension of the scalar approach of the previous section, where the target now is the description of the symmetries of the deformations and forces. Use of our previous assumption of replication of behaviour within the unit cell under translation implies that we do not have to deal with the infinite group $\mathcal{G}$, and instead we can restrict consideration to the *factor group* $\mathcal{P} = \mathcal{G}/\mathcal{T}$, where $\mathcal{T}$ is the group of translations in the appropriate dimension. The factor group is isomorphic to a point group [15]. This fact allows us to capture interesting additional information regarding symmetry with an extension of the approach used for finite structures.

Scalar equation (2.1) for the net mobility $m - s$ has terms relating to the freedom of the joints, the constraints imposed by the bars, the deformation modes of the unit cell and rigid-body translations. The symmetry-extended version of this equation is

$$\text{(two or three dimensions)} \quad \Gamma(m) - \Gamma(s) = \Gamma(j) \times \Gamma_{\mathrm{T}} - \Gamma(b) + \Gamma_{\mathrm{def}} - \Gamma_{\mathrm{T}}, \tag{3.1}$$

where the new term Γ_{def} collects the character of the infinitesimal deformations of the unit cell. These deformations can be described by a symmetric second-order tensor, and hence span the symmetry $[\Gamma_{\mathrm{T}}^2]$, the symmetric part of the product $\Gamma_{\mathrm{T}} \times \Gamma_{\mathrm{T}}$ [16]. As the antisymmetric part of the square is $\{\Gamma_{\mathrm{T}}^2\} = \Gamma_{\mathrm{R}}$, we have

$$\text{(two or three dimensions)} \quad \Gamma_{\mathrm{def}} = \Gamma_{\mathrm{T}} \times \Gamma_{\mathrm{T}} - \Gamma_{\mathrm{R}}. \tag{3.2}$$

Hence, the symmetry-extended Maxwell equation for periodic bar-and-joint frameworks is

$$\text{(two or three dimensions)} \quad \Gamma(m) - \Gamma(s) = \Gamma(j) \times \Gamma_{\mathrm{T}} - \Gamma(b) + \Gamma_{\mathrm{T}} \times \Gamma_{\mathrm{T}} - \Gamma_{\mathrm{T}} - \Gamma_{\mathrm{R}}, \tag{3.3}$$

with Γ_{T} and Γ_{R} defined for two dimensions and three dimensions as in (1.3), and all representations calculated in the factor group $\mathcal{P}$. This equation expresses our main result for periodic bar-and-joint frameworks in two dimensions and three dimensions. It gives an explicit expression for the numbers and symmetries of the mechanisms and states of self-stress in terms of the numbers and symmetries of components of the framework.

Note that the role of the point group is somewhat different in the treatment of finite and periodic frameworks. In the finite case, the point group is the symmetry group of the object under consideration. In the periodic case, the point group arises only because it is isomorphic to the factor group. A corresponding element may therefore have a different physical significance in each group. For example, in two dimensions there may be multiple centres of rotation, and in three dimensions it may be that not all rotation axes pass through a common point. 'Reflection' operations of the point group may correspond to glide reflections in the factor group, and 'rotations' to screw rotations in the factor group.

In our examples, we use Hermann–Mauguin notation for the space groups/plane groups, and Schoenflies notation for the point group isomorphic to the factor group, which we often loosely call just 'the point group'.

In general, the result for $\Gamma(m) - \Gamma(s)$ obtained from (3.3) will depend on the size and location of the unit cell. Effectively, the choice of unit cell corresponds to a decision to work within a particular finite subgroup of the original infinite space group. We cannot tell in advance which choice of unit cell might lead to interesting behaviour; what we are doing here is to give the machinery for making the calculation once the unit cell is chosen. The system shown later in figure 6 (analysed in §6) is an example where the correct choice of unit cell is important for the detection of a mechanism.

4. Examples for bar-and-joint frameworks

(a) A two-dimensional bar-and-joint framework: the kagome framework

The plane group of the kagome framework is $p6m$, and the point group isomorphic to the factor group is C_{6v} [15]. Simple counting gives $2j - b + 1 = 1$, indicating that the framework is locally isostatic [14], having at least one mechanism that repeats identically in every unit cell. Application of (3.3) in a tabular form showing the character under each symmetry operation, and using the Mulliken notation [17] for each representation, gives

C_{6v}	E	$2C_6$	$2C_3$	C_2	$3\sigma_v$	$3\sigma_d$	
$\Gamma(j)$	3	0	0	3	1	1	$A_1 + E_2$
$\times\Gamma_{\mathrm{T}}$	2	1	−1	−2	0	0	E_1
$=$	6	0	0	−6	0	0	$B_1 + B_2 + 2E_1$
$-\Gamma(b)$	−6	0	0	0	−2	0	$-A_1 - B_1 - E_1 - E_2$
$=$	0	0	0	−6	−2	0	$-A_1 + B_2 + E_1 - E_2$
$+\Gamma_{\mathrm{T}}^2$	4	1	1	4	0	0	$A_1 + A_2 + E_2$
$-\Gamma_{\mathrm{T}}$	−2	−1	1	2	0	0	$-E_1$
$-\Gamma_{\mathrm{R}}$	−1	−1	−1	−1	1	1	$-A_2$
$\Gamma(m) - \Gamma(s)$	1	−1	1	−1	−1	1	B_2

This tabulation and those in the examples that follow set out the calculation in a standard form that was devised for [3] and used in subsequent papers. The general arrangement is similar to that used in chemical applications of point group theory, such as the calculation of symmetry properties of molecular vibrations [16,18]. Some brief remarks about the notation may be useful. The first line gives the point group (denoted by the Schoenflies symbol) and lists by classes the different symmetry operations that constitute the group. In general, operations S have symbols drawn from the set of: E for the identity, C_n for a proper rotation by $2\pi/n$ (subscripted with prime(s) to avoid ambiguity when a C_2 rotation is performed about an axis at right angles to the axis of the highest order), i for the inversion, S_n for an improper rotation (a rotation through $2\pi/n$ followed by a reflection in the plane perpendicular to the axis) and σ for reflection in a mirror plane (with a descriptive label such as v, h, d to distinguish vertical, horizontal, dihedral planes). Settings of the point groups and the definitions of the various distinguishing labels are given in [16,18,19]. The final column of the table shows the reduction of the row of traces $\chi(S)$ to a direct sum of irreducible representations of the point group. The notation for these follows Mulliken, as noted earlier: representations are labelled A (non-degenerate, symmetric under C_n rotation about the principal axis), B (non-degenerate, antisymmetric under C_n rotation about the principal axis), E (doubly degenerate) or T (triply degenerate) and distinguished by subscripts and superscripts as necessary, such as g/u subscripts for symmetry/antisymmetry under inversion, single and double prime superscripts for symmetry under horizontal planes and so on. These standard labellings are to be found in compilations of character tables for chemistry [16,19].

Returning to the specific example of the kagome framework, the calculation shown in the table above has identified the symmetry of the mechanism predicted by the scalar count. This mechanism has B_2 symmetry. Note that the one-dimensional B_2 representation: (i) is present in only one copy in $\Gamma(j) \times \Gamma_{\mathrm{T}}$, (ii) is not present in $\Gamma(b)$, and (iii) is not present in $\Gamma_{\mathrm{T}}^2 - \Gamma_{\mathrm{R}}$. Observations (i) and (ii) imply that the mechanism is uniquely defined by the symmetry, and, by (iii), does not require any deformation of the unit cell. The motion associated with the mechanism consists of alternating rotations of triangular units; the sense of rotation of any triangle is opposite to that of its three neighbours, as shown in figure 2*d*.

This example has illustrated the way that counting with symmetry can, in favourable cases, give not only the symmetry but also an explicit definition of the mechanism. In the particular case of the kagome lattice, the symmetry-detectable mechanism is known from numerical calculations to be unique under the constraint that the contents of all unit cells are defined by translation. Thus, the symmetry-extended Maxwell rule (5.5) gives a complete solution in this case.

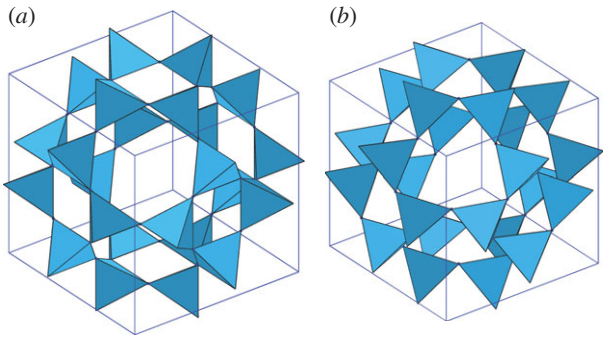

Figure 3. The 'sodalite' framework. (*a*) The fully expanded maximum symmetry framework appropriate to the synthetic soda-1 structure. The unit cell used in the mobility calculation is indicated by thin lines, and for clarity the tetrahedra are shown as solid bodies. (*b*) A deformed configuration of the framework which corresponds to the pure A_{2u} rotational collapse mode, and closely models the experimental structure of mineral sodalite [20]. A rotation of 23° was applied to all tetrahedra in (*a*) to yield (*b*). This value is near to the average of the angles reported in [22] for SiO_4 and AlO_4 tetrahedra in the mineral; it leads to shrinkage of the side length of the unit cell by a factor of 0.92. (Online version in colour.)

(b) A three-dimensional bar-and-joint framework: the 'sodalite' framework

Sodalite is a dark blue mineral of formula $Na_8Cl_2Al_6Si_6O_{24}$ [20] of space group $P\bar{4}3n$ and point group T_d. The crystal structure is built from SiO_4 and AlO_4 tetrahedra, linked by corner-sharing of oxygen atoms. The experimentally observed structure can be considered to result from distortion of a predecessor of higher symmetry by a process that was termed 'rotational collapse' by Pauling in his early studies of the X-ray diffraction pattern of this compound [21]. Concerted rotation of the tetrahedra is accompanied by small distortions in edge lengths and variations in rotational angle between chemically different tetrahedra [22].

For the present application, we consider an idealized framework based on sodalite, in which the MO_4 units are modelled as regular tetrahedra [23,24]. In our bar-and-joint model, a bar is placed along each tetrahedron edge, and a spherical joint is placed at each tetrahedron vertex (oxygen position). Six bars meet at each joint, three from each of two neighbouring tetrahedra. We take all bars to have the same length, thereby removing the distinction between SiO_4 and AlO_4, which raises the symmetry to $I\bar{4}3m$ [25], which also has point group T_d. We now consider the fully expanded structure, which further raises the space group symmetry to the topological symmetry of the framework, i.e. $Im\bar{3}m$, with point group O_h. With these restrictions, the framework is a model for the unsubstituted silica sodalite $Si_{12}O_{24}$, which does not occur naturally, but has been made by template synthesis [26,27]. This is the 'soda-1' structure studied in [20]. The relationship between various sodalite-like frameworks has been described in [28]. The point group of our idealized structure (shown in figure 3) is O_h. The unit cell contains 24 joints and 72 bars, and scalar counting using (2.1) gives $m - s = 3$. Application of (3.3) in tabular form is given in table 1.

From the form of the reducible representation $\Gamma(m) - \Gamma(s)$ in the final row of the table, we can deduce that there are at least seven mechanisms that repeat identically in every unit cell and that these span $A_{2u} + T_{1g} + 2T_{2g}$. Symmetry has clearly already revealed more mechanisms than the scalar count; it also gives an important clue to the deformation modes of this crystal framework. The non-degenerate A_{2u} mechanism breaks the inversion symmetry, and if we follow this distortion mode we arrive at the space group $I\bar{4}3m$ with point group T_d. In the lower group, $\Gamma(m) - \Gamma(s) = A_1 + 2T_2 - 2A_2 - E$; hence, in the absence of totally symmetric states of self-stress, undetected in the higher symmetry group, the mechanism is finite [29] and becomes totally symmetric in the lower group. The mechanism consists of concerted rotations of tetrahedra and follows the 'rotational collapse' mode described by Pauling [21], and this distortion of the model pin-jointed framework takes it close to the experimental structure of mineral sodalite. Although

Table 1. Tabular calculation of $\Gamma(m) - \Gamma(s)$ for the high-symmetry sodalite lattice illustrated in figure 3*a*.

O_h	E	$8C_3$	$6C_2$	$6C_4$	$3C_4^2$	i	$6S_4$	$8S_6$	$3\sigma_h$	$6\sigma_d$	
$\Gamma(j)$	24	0	4	0	0	0	0	0	8	4	$2A_{1g} + 2E_g + 2T_{2g} + 2T_{1u} + 2T_{2u}$
$\times\Gamma_\mathrm{T}$	3	0	−1	1	−1	−3	−1	0	1	1	T_{1u}
$=$	72	0	−4	0	0	0	0	0	8	4	$2A_{1g} + 2A_{2g} + 4E_g + 4T_{1g} + 4T_{2g} + 2A_{2u} + 2E_u + 6T_{1u} + 4T_{2u}$
$-\Gamma(b)$	−72	0	0	0	−8	0	0	0	−16	0	$-3A_{1g} - 3A_{2g} - 6E_g - 3T_{1g} - 3T_{2g} - A_{1u} - A_{2u} - 2E_u - 5T_{1u} - 5T_{2u}$
$=$	0	0	−4	0	−8	0	0	0	−8	4	$-A_{1g} - A_{2g} - 2E_g + T_{1g} + T_{2g} - A_{1u} + A_{2u} + T_{1u} - T_{2u}$
$+\Gamma_\mathrm{T}^2$	9	0	1	1	1	9	1	0	1	1	$A_{1g} + E_g + T_{1g} + T_{2g}$
$-\Gamma_\mathrm{T}$	−3	0	1	−1	1	3	1	0	−1	−1	$-T_{1u}$
$-\Gamma_\mathrm{R}$	−3	0	1	−1	1	−3	−1	0	1	1	$-T_{1g}$
$\Gamma(m) - \Gamma(s)$	3	0	−1	−1	−5	9	1	0	−7	5	$A_{2u} + T_{1g} + 2T_{2g} - A_{2g} - E_g - A_{1u} - T_{2u}$

the mechanism follows a continuous geometrical path, in practice it will ultimately be blocked by steric constraints of the kind invoked in more detailed descriptions of the crystal structure [20].

5. Periodic mobility counting for body-and-joint models

In the analysis of finite structures, it is sometimes convenient to consider assemblies of bodies connected by joints rather than assemblies of joints connected by rigid bars. In the body-and-joint model, the rigid bodies are typically polygonal or polyhedral and the joints may be of general type. This approach is also useful in the world of repetitive structures. Solid-state materials are often modelled in terms of rigid tetrahedral and octahedral units [30]. In the present section, we derive symmetry-extended counting rules for the mobility of periodic structures treated in this alternative body-and-joint model.

Scalar counting of the relative degrees of freedom, or mobility, of a mechanical linkage consisting of n bodies connected by g joints, where joint i permits f_i relative freedoms is [5,6]

$$\left.\begin{aligned} &\text{(two dimensions)} \quad m - s = 3(n-1) - 3g + \sum_{i=1}^{g} f_i \\ \text{and} \quad &\text{(three dimensions)} \quad m - s = 6(n-1) - 6g + \sum_{i=1}^{g} f_i. \end{aligned}\right\} \tag{5.1}$$

The terms on the RHS account, respectively, for the overall freedoms of all n bodies minus the rigid-body motions of the assembly, the constraints imposed by rigidly glued joints, and the restoration of the actual freedoms of the joints.

Conversion of (5.1) to allow for periodicity is straightforward. First, the rigid-body motions are restored, then the freedoms associated with the deformations of the unit cell are added, and finally the appropriate rigid-body displacements are removed. The net effect is to add four to the RHS of the two-dimensional equation or nine to the RHS of the three-dimensional equation, as for the pin-jointed case (2.1), leaving, for periodic systems,

$$\left.\begin{aligned} &\text{(two dimensions)} \quad m - s = 3n - 3g + \sum_{i=1}^{g} f_i + 1 \\ \text{and} \quad &\text{(three dimensions)} \quad m - s = 6n - 6g + \sum_{i=1}^{g} f_i + 3. \end{aligned}\right\} \tag{5.2}$$

For two-dimensional periodic linkages where all joints are pin joints, we have $f_i = 1$ for all i, and for three-dimensional periodic linkages where all joints are spherical joints we have $f_i = 3$ for all i, and hence (5.2) becomes

$$\left.\begin{aligned} &\text{(two dimensions)} \quad m - s = 3n - 2g + 1 \\ \text{and} \quad &\text{(three dimensions)} \quad m - s = 6n - 3g + 3. \end{aligned}\right\} \tag{5.3}$$

In the symmetry extension of the mobility criterion for finite frameworks, it is useful to consider the 'contact polyhedron' C, which has vertices that represent the rigid elements of the structure and has edges that represent the joints. The expression is derived from a thought experiment where the structure is first considered to be a rigid assembly with all joints glued, and the joint freedoms are then restored. The result is, from [6],

$$\text{(two or three dimensions)} \quad \Gamma(m) - \Gamma(s) = (\Gamma(v,C) - \Gamma_{\parallel}(e,C) - \Gamma_0) \times (\Gamma_{\mathrm{T}} + \Gamma_{\mathrm{R}}) + \Gamma_{\text{freedoms}}, \tag{5.4}$$

where now $\Gamma(v,C)$ is the permutation representation of the vertices of C, $\Gamma_{\parallel}(e,C)$ is the representation of the set of vectors directed along the edges of C, and Γ_{freedoms} is the representation of the freedoms of the joints. The detailed structure of Γ_{freedoms} depends on the types and distributions of the joints. Conversion of (5.4) for periodic structures follows the same route as the extension of (1.2) to (3.3), i.e. addition of the same fourfold

(two-dimensional)/ninefold (three-dimensional) reducible representations $\Gamma_T \times \Gamma_T$ to the RHS, leaving, for periodic systems,

$$\text{(two or three dimensions)} \quad \Gamma(m) - \Gamma(s) = (\Gamma(v,C) - \Gamma_{\parallel}(e,C) - \Gamma_0) \times (\Gamma_T + \Gamma_R) + \Gamma_{\text{freedoms}} + \Gamma_T \times \Gamma_T \tag{5.5}$$

with Γ_T as given in (1.3). The contact 'polyhedron' is now infinite but we consider its restriction to the unit cell or, more formally, its quotient with respect to translations.

Specialization to the case of all pin joints (two dimensions) or all spherical joints (three dimensions) relies on [6]

$$\text{(two or three dimensions)} \quad \Gamma_{\text{freedoms}} = \Gamma_{\parallel}(e,C) \times \Gamma_R \tag{5.6}$$

and hence the explicit formula for periodic structures of this simplified type is

$$\text{(two or three dimensions)} \quad \Gamma(m) - \Gamma(s) = \Gamma(v,C) \times (\Gamma_T + \Gamma_R) - \Gamma_{\parallel}(e,C) \times \Gamma_T + \Gamma_T \times \Gamma_T - \Gamma_T - \Gamma_R, \tag{5.7}$$

where the three terms on the RHS encapsulate the freedoms, constraints and periodicity effects that contribute to the net mobility of the structure.

6. Examples for body-and-joint structures

The kagome and sodalite calculations of §4 can be reworked in terms of rigid triangular plates and rigid tetrahedral bodies. The results for $\Gamma(m) - \Gamma(s)$ from (5.7) for any particular system will be identical to those from the bar-and-joint analysis using (3.3). This correspondence is guaranteed by the presence of rigid simplices of bars within the bar-and-joint version of the framework.

(a) Infinite frameworks of pin-jointed rectangles

Body-and-joint mobility criterion (5.7) is ideally suited to analysis of the hinged polygon constructions that are common in the literature of auxetic materials [31,32]. One system that has been studied in detail in connection with the explanation of auxetic behaviour in two dimensions is built on the square lattice. Symmetry calculations on three variants of this basic system are treated here.

The first model [32] consists of a lattice of rectangles of two sizes, pinned together at their corners. In the highest-symmetry realization, this structure belongs to the plane group $p2mm$ with point group C_{2v}. The calculation using (5.7) with the unit cell shown in figure 4 is

C_{2v}	E	C_2	$2\sigma_x$	$2\sigma_y$	
$\Gamma(v,C)$	2	2	2	2	$2A_1$
$\times(\Gamma_T + \Gamma_R)$	3	−1	−1	−1	$A_2 + B_1 + B_2$
$=$	6	−2	−2	−2	$2A_2 + 2B_1 + 2B_2$
$-\Gamma_{\parallel}(e,C)$	−4	0	0	0	$-A_1 - B_1 - E_1 - B_1$
$\times\Gamma_T$	2	−2	0	0	$B_1 + B_2$
$=$	−8	0	0	0	$-2A_1 - 2A_2 - 2B_1 - 2B_2$
$\Gamma_T^2 - \Gamma_R$	1	5	1	1	$2A_1 + A_1 - B_1 - B_2$
$\Gamma(m) - \Gamma(s)$	−1	3	−1	−1	$A_2 - B_1 - B_2$

Scalar counting (5.3) gives $m - s = -1$, showing only that the system is overconstrained. The symmetry calculation reveals that the net count of -1 conceals one mechanism and two states of self-stress. Further, the A_2 mechanism is finite in the absence of an equisymmetric state of self-stress, as a necessary consequence of the Abelian nature of C_{2v}. As Grima *et al.* [32] comment, this mechanism is auxetic.

In the case where the rectangles degenerate to squares of two different sizes, we recover the system considered by Grima & Evans [31]. The plane group is now $p4mm$ and the point group is

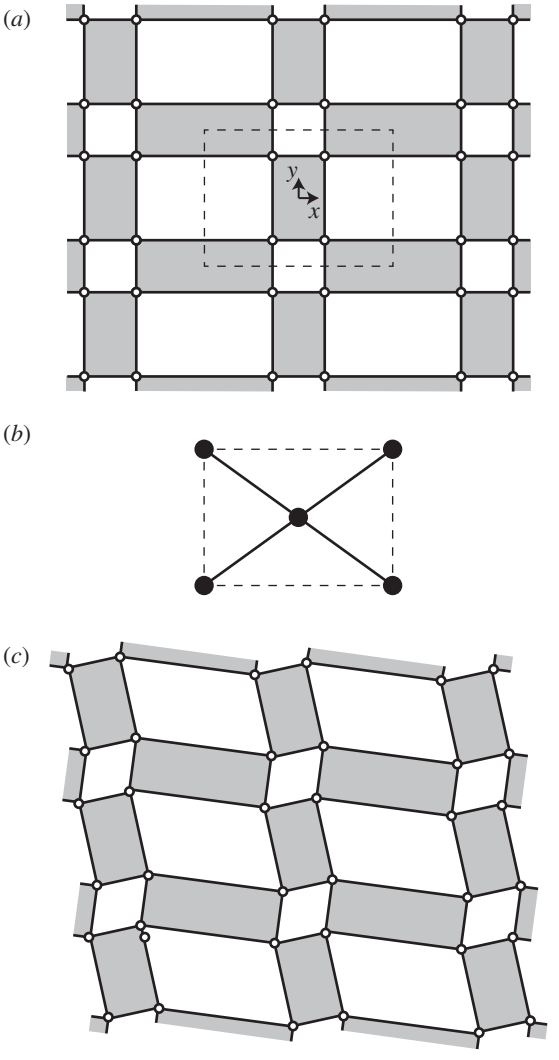

Figure 4. Model for an auxetic material based on rectangles of two sizes, showing (*a*) the model and the choice of unit cell with rigid plates indicated by shading; (*b*) the contact polyhedron *C* for the unit cell; and (*c*) a deformed configuration, illustrating the A_2-symmetric mechanism.

C_{4v} with mirror lines d running both vertically and horizontally in the (now square) unit cell, and the mirror lines v running diagonally. In this case, construction of a bar-and-joint model consistent with the symmetry would require each square to be braced across both diagonals, generating an unwanted local state of self-stress. This is avoided for the body-and-hinge model, for which the symmetry calculation gives

C_{4v}	E	$2C_4$	C_2	$2\sigma_v$	$2\sigma_d$	
$\Gamma(v,C)$	2	2	2	2	2	$2A_1$
$\times(\Gamma_T+\Gamma_R)$	3	1	−1	−1	−1	A_2+E
$=$	6	2	−2	−2	−2	$2A_1+2+2E$
$-\Gamma_{\|}(e,C)$	−4	0	0	−2	0	$-A_1-B_1-E$
$\times\Gamma_T$	2	0	−2	0	0	E
$=$	−8	0	0	0	0	$-A_1-A_2-B_1-B_2-2E$
$\Gamma_T^2-\Gamma_R$	1	−1	5	1	1	$A_1+B_1+B_2-E$
$\Gamma(m)-\Gamma(s)$	−1	1	3	−1	−1	A_2-E

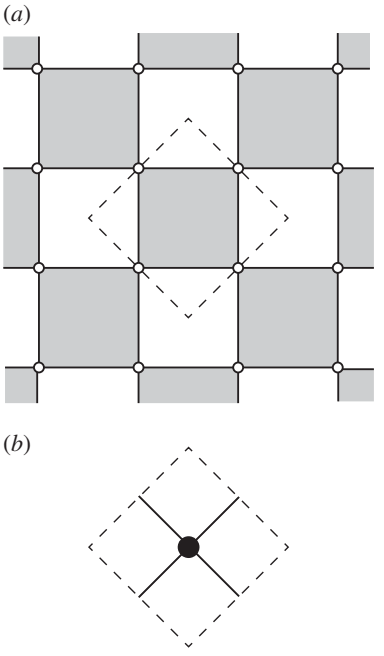

Figure 5. Model for an auxetic material based on squares of equal size, showing (*a*) the model and the smallest choice of unit cell with rigid plates indicated by shading and (*b*) the contact polyhedron *C* for the unit cell which in this case consists of a single unique vertex.

Clearly, the scalar count (5.3) is unchanged by the symmetrization of the rectangles, and the only change in $\Gamma(m) - \Gamma(s)$ is the collapse of the B_1 and B_2 pair of states of self-stress to a degenerate E pair. The physical conclusions about the continuous nature of the mechanism are unchanged.

In the further limiting case when the two squares become equal in size, a smaller unit cell becomes possible, as shown in figure 5. Straightforward application of (5.7) gives

C_{4v}	E	$2C_4$	C_2	$2\sigma_v$	$2\sigma_d$	
$\Gamma(v,C)$	1	1	1	1	1	A_1
$\times(\Gamma_T + \Gamma_R)$	3	1	−1	−1	−1	$A_2 + E$
$=$	3	1	−1	−1	−1	$A_1 + A_2 + E$
$-\Gamma_{\|}(e,C)$	−2	0	2	0	0	$-E$
$\times\Gamma_T$	2	0	−2	0	0	E
$=$	−4	0	−4	0	0	$-A_1 - A_2 - B_1 - B_2$
$\Gamma_T^2 - \Gamma_R$	1	−1	5	1	1	$A_1 + B_1 + B_2 - E$
$\Gamma(m) - \Gamma(s)$	0	0	0	0	0	0

Thus, in this case, neither the scalar count nor the symmetry count gives any indication of the mobility that we know to be present from the previous calculation. The physical explanation of this apparent paradox is clear; by assumption of the smaller unit cell, we have constrained every square to behave in the same way and this is inconsistent with the counter-rotating nature of the mechanism.

This example illustrates the potential pitfalls of fixing a unit cell in advance. Mechanisms will be discovered by this method only if they break symmetry and are consistent with a fixed unit cell. Figure 6 shows twelve different unit cells, each of which may give different results for $\Gamma(m) - \Gamma(s)$, reflecting the different states of self-stress and mechanisms that are consistent with the subgroup of the space group that is implied by the choice of unit cell.

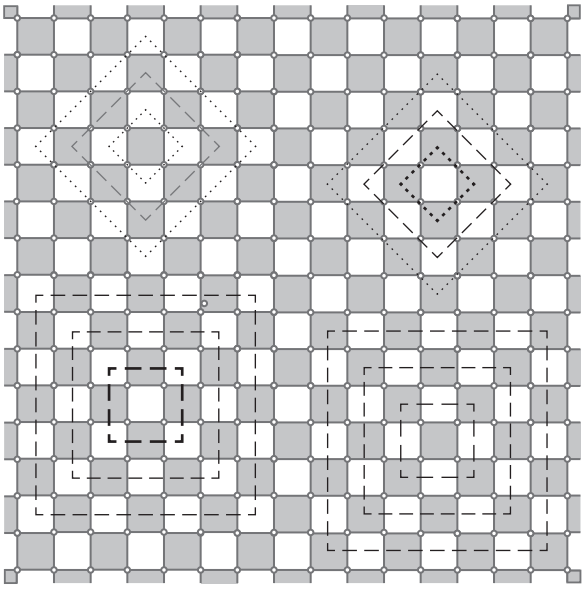

Figure 6. Twelve different choices of unit cell for an auxetic material based on squares of equal size. The unit cells marked with dotted (rather than dashed) lines are inconsistent with the mechanism in which alternate squares rotate in opposite directions. The two unit cells marked in bold are analysed by tabular calculation in the text.

7. A symmetry-extended notion of local isostaticity

An isostatic framework is one that has neither mechanisms nor states of self-stress. A necessary scalar condition for isostaticity is $m - s = 0$, which is the character under the identity of the stronger condition $\Gamma(m) - \Gamma(s) = 0$ which demands cancellation under all symmetry operations [33]. For periodic systems this condition is impossible to attain [12], but Kapko *et al.* [14] introduced the concept of 'locally isostatic' to denote situations where, on average, the number of constraints balance out the number of freedoms. Hence, for a locally isostatic two-dimensional periodic framework, $b - 2j$ and $m - s = 1$ by (2.1). The equality $b = 2j$ (equivalently, $b = 3j$ in three dimensions) is again effectively the character under the identity of a symmetry relationship,

$$\Gamma(b) = \Gamma(j) \times \Gamma_{\mathrm{T}}. \tag{7.1}$$

Suppose that we insist that (7.1) holds, i.e. that $\chi_b(S) = \chi_j(S)\chi_T(S)$ for all S. Then, by (3.3),

$$\Gamma(m) - \Gamma(s) = \Gamma_{\mathrm{T}} \times \Gamma_{\mathrm{T}} - \Gamma_{\mathrm{T}} - \Gamma_{\mathrm{R}}, \tag{7.2}$$

which is a stronger symmetry condition for an extended notion of local isostaticity. In two dimensions, (7.2) leads to some interesting conclusions about the possible placement of structural components of the periodic framework. The conditions for the vanishing of the character of $\Gamma(m) - \Gamma(s)$ for the different allowed operations R are, in two dimensions:

$$\left.\begin{aligned} \chi(E): &\quad 2j = b, \\ \chi(C_2): &\quad -2j_2 = b_2, \\ \chi(C_3): &\quad -j_3 = b_3, \\ \chi(C_4): &\quad 0j_4 = b_4, \\ \chi(C_6): &\quad j_6 = b_6 \end{aligned}\right\} \tag{7.3}$$

and

$$\chi(\sigma): \quad 0j_\sigma = b_\sigma,$$

where b_N and j_N are, respectively, the number of bars and joints lying on a C_N axis, and b_σ and j_σ are, respectively, the number of bars and joints preserved by a σ mirror. As each of these counts is non-negative, we can deduce that $j_2 = j_3 = 0$, $b_2 = b_3 = b_4 = b_\sigma = 0$. Further, as no bar can be preserved by a C_N operation with $N > 2$, $b_6 = 0$ and hence $j_6 = 0$. In addition, as any joint on a C_4 axis must also lie on a C_2 axis, $j_2 \geq j_4$ and as $j_2 = 0$, j_4 must also be 0. The value of j_σ is unrestricted. Hence, a two-dimensional locally isostatic periodic framework with j joints and $2j$ bars has joints only in general position, in mirror lines, or in both, and has bars in general position only. If all joints are also in general position, we have

$$\Gamma_j = \frac{j}{|G|}\Gamma_{\mathrm{reg}}; \quad \Gamma_b = \frac{2j}{|G|}\Gamma_{\mathrm{reg}}, \tag{7.4}$$

where $|G|$ is the order of the point group, and Γ_{reg} is the regular representation, with $\chi_{\mathrm{reg}}(E) = |G|$, and $\chi_{\mathrm{reg}}(R) = 0$ for $R \neq E$; trivially, $\Gamma_j \times \Gamma_{\mathrm{T}} - \Gamma(b) = 0$ in this case.

There is a distinction between scalar and symmetry-extended notions of local isostaticity. The latter is more restrictive, and may depend on the choice of unit cell. For instance, the kagome lattice is 4-regular, and hence has $m - s = 1$. However, the symmetry calculation with the minimum unit cell used in §4*a* gives

$$\begin{aligned}\Gamma(j) \times \Gamma_{\mathrm{T}} - \Gamma(b) &= (B_1 + B_2 + 2E_1) - (A_1 + B_1 + E_1 + E_2)\\ &= -A_1 + B_2 + E_1 - E_2\end{aligned} \tag{7.5}$$

in the C_{6v} point group. The operations for which the framework departs from the local isostatic count are $S = C_2$, where $j_2 = 3$, and the mirror σ, where $b_\sigma = 1$. Once the system has distorted along the B_2 mode, the plane group is reduced to $p31m$ with point group C_{3v} and the RHS of (7.5) vanishes. Only then has the system attained locally isostatic status on both scalar and symmetry-extended criteria. Considered in terms of characters in the distorted configuration, as the mirror lines run parallel with the bars, but pass through joints and hexagon centres, $b_\sigma = 0$ and $j_\sigma = 2$. In addition, the C_3 axes lie at the centres of triangles and hexagons, and hence $j_3 = b_3 = 0$, consistent with (7.3). Indeed, in this case, for any unit cell consisting of $n \times n$ copies of the one shown in figure 2*d*, the counts will become $b_\sigma = 0$, $j_3 = b_3 = 0$, with $j_\sigma = 2n$, showing that the distorted kagome lattice with space group $p31m$ is locally isostatic for *any* choice of unit cell.

Acknowledgements. We thank Holger Mitschke (Universität Erlangen-Nürnberg) for helpful discussions during the drafting of this paper. P.W.F. thanks the Royal Society and Leverhulme Trust for a Senior Research Fellowship.

References

1. Maxwell JC. 1864 On the calculation of the equilibrium and stiffness of frames. *Philos. Mag.* **27**, 294–299.
2. Calladine CR. 1978 Buckminster Fuller's 'Tensegrity' structures and Clerk Maxwell's rules for the construction of stiff frames. *Int. J. Solids Struct.* **14**, 161–172. (doi:10.1016/0020-7683(78)90052-5)
3. Fowler PW, Guest SD. 2000 A symmetry extension of Maxwell's rule for rigidity of frames. *Int. J. Solids Struct.* **37**, 1793–1804. (doi:10.1016/S0020-7683(98)00326-6)
4. Grübler M. 1917 *Getriebelehre*. Berlin, Germany: Springer.
5. Kutzbach K. 1929 Mechanische leitungsverzweigung. *Maschinenbau, Der Betrieb* **8**, 710–716.
6. Guest SD, Fowler PW. 2005 A symmetry-extended mobility rule. *Mech. Mach. Theory* **40**, 1002–1014. (doi:10.1016/j.mechmachtheory.2004.12.017)
7. Ross E, Schulze B, Whiteley W. 2011 Finite motions from periodic frameworks with added symmetry. *Int. J. Solids Struct.* **48**, 1711–1729. (doi:10.1016/j.ijsolstr.2011.02.018)
8. Malestein J, Theran L. 2012 Generic rigidity with forced symmetry and sparse colored graphs. (http://arxiv.org/abs/1203.0772)
9. Dove MT. 2005 *Introduction to lattice dynamics*. Cambridge, UK: Cambridge University Press.
10. Borcea CS, Streinu S. 2010 Periodic frameworks and flexibility. *Proc. R. Soc. A* **466**, 2633–2649. (doi:10.1098/rspa.2009.0676)

11. Timoshenko SP, Goodier JN. 1969 *Theory of elasticity*, 3rd edn. New York, NY: McGraw-Hill.
12. Guest SD, Hutchinson JW. 2003 On the determinacy of repetitive structures. *J. Mech. Phys. Solids* **51**, 383–391. (doi:10.1016/S0022-5096(02)00107-2)
13. Owen JC, Power SC. 2011 Infinite bar-joint frameworks, crystals and operator theory. *N.Y. J. Math.* **17**, 445–490.
14. Kapko V, Treacy MMJ, Thorpe MF, Guest SD. 2009 On the collapse of locally isostatic networks. *Proc. R. Soc. A* **465**, 3517–3530. (doi:10.1098/rspa.2009.0307)
15. Burns G, Glazer AM. 1990 *Space groups for solid state scientists*, 2nd edn. San Diego, CA: Academic Press.
16. Atkins PW, Child MS, Phillips CSG. 1970 *Tables for group theory*. Oxford, UK: Oxford University Press.
17. Mulliken RS. 1955 Report on notation for the spectra of polyatomic molecules. *J. Chem. Phys.* **23**, 1997–2011. (doi:10.1063/1.1740655)
18. Bishop DM. 1973 *Group theory and chemistry*. Oxford, UK: Clarendon Press.
19. Altmann SL, Herzig P. 1994 *Point-group theory tables*. Oxford, UK: Clarendon Press.
20. Thomson KT, Wentzcovitch RM, McCormick A, Davis HT. 1998 A density functional study of sodalite: a new view on an old system. *Chem. Phys. Lett.* **283**, 39–43. (doi:10.1016/S0009-2614(97)01342-0)
21. Pauling L. 1930 The structure of sodalite and helvite. *Z. Kristallogr.* **74**, 213–225.
22. Hassan I, Grundy HD. 1984 The crystal structures of sodalite-group minerals. *Acta Crystallogr. B* **40**, 6–13. (doi:10.1107/S0108768184001683)
23. Sartbaeva A, Wells S, Treacy MMJ, Thorpe MF. 2006 The flexibility window in zeolites. *Nat. Mater.* **5**, 962–965. (doi:10.1038/nmat1784)
24. Power SC. 2013 Polynomials for crystal frameworks and the rigid unit mode spectrum. (http://arxiv.org/abs/1102.2744)
25. Depmeier W. 1992 Remarks on symmetries occurring in the sodalite family. *Z. Kristallogr.* **199**, 75–89. (doi:10.1524/zkri.1992.199.1-2.75)
26. Bibby DM, Dale MP. 1985 Synthesis of silica-sodalite from non-aqueous systems. *Nature* **317**, 157–158. (doi:10.1038/317157a0)
27. Richardson Jr JW, Pluth JJ, Smith JV, Dytrych WJ, Bibby DM. 1988 Conformation of ethylene glycol and phase change in silica sodalite. *J. Phys. Chem.* **92**, 243–247. (doi:10.1021/j100312a052)
28. Fischer RX, Baur WH. 2009 Symmetry relationships of sodalite (SOD)-type crystal structures. *Z. Kristallogr.* **224**, 185–197. (doi:10.1524/zkri.2009.1147)
29. Guest SD, Fowler PW. 2007 Symmetry conditions and finite mechanisms. *J. Mech. Mater. Struct.* **2**, 293–301. (doi:10.2140/jomms.2007.2.293)
30. Giddy AP, Dove MT, Pawley GS, Heine V. 1993 The determination of rigid-unit modes as potential soft modes for displacive phase transitions in framework crystal structures. *Acta Crystallogr. A* **49**, 697–703. (doi:10.1107/S0108767393002545)
31. Grima JN, Evans KE. 2000 Auxetic behaviour from rotating squares. *J. Mater. Sci. Lett.* **19**, 1563–1565. (doi:10.1023/A:1006781224002)
32. Grima JN, Manicaro E, Attard D. 2011 Auxetic behaviour from connected different-size squares and rectangles. *Proc. R. Soc. A* **467**, 439–458. (doi:10.1098/rspa.2010.0171)
33. Connelly R, Fowler PW, Guest SD, Schulze B, Whiteley WJ. 2009 When is a symmetric pin-jointed framework isostatic? *Int. J. Solids Struct.* **46**, 762–773. (doi:10.1016/j.ijsolstr.2008.09.023)